Computers and Electronics in Agriculture 214 (2023) 108300

Contents lists available at ScienceDirect

Computers and Electronics in Agriculture

journal homepage: www.elsevier.com/locate/compag

On space–time ratio in the soybean mass aeration problem using a manufactured solution with realistic parameters

Daniel Rigoni [a,b,*], Marcio A.V. Pinto [c], Jotair E. Kwiatkowski Jr [b,d]

[a] Department of Mathematics, State University of Central-West, 85040-167 Guarapuava, PR, Brazil
[b] Graduate Program in Numerical Methods in Engineering, Federal University of Paraná, 81531-980 Curitiba, PR, Brazil
[c] Department of Mechanical Engineering, Federal University of Paraná, 81531-980 Curitiba, PR, Brazil
[d] Department of Computer Science, State University of Central-West, 85040-167 Guarapuava, PR, Brazil

ARTICLE INFO

Keywords:
Space-time ratio
Postharvest
Grain Storage
Thorpe
Finite Difference Method

ABSTRACT

The purpose of this paper is to introduce a new manufactured analytical solution to the mathematical model that describes the behavior of the grain mass aeration process, proposed by Thorpe, using the method of manufactured solutions. The finite difference method, utilizing the CDS-Crank-Nicolson and Leith's methods, was employed. An error analysis of the approximations used was performed to verify the effective and apparent orders of the discretization error obtained with mesh refinement. Furthermore, a study on the space–time ratio in the numerical methods was carried out in two realistic settings of soybeans aeration process. It was observed that Leith's method outperformed the CDS-Crank-Nicolson method. Therefore, Leith's method is recommended by this paper to numerically solve the grain mass aeration model proposed by Thorpe, given its robustness with respect to the space–time ratio in both settings studied.

1. Introduction

In the 2020 harvest, global soybean production was 337.298 million tons, with Brazil and the United States being responsible for 65.68% of this production (FAO, 2020). Soybeans are mainly used in the petroleum and protein industries, but they are not immediately processed, so storage for extended periods is required (Cañizares et al., 2021).

Soybeans are a living organism and therefore have an active metabolism still in the postharvest stage. During this stage, factors such as temperature and moisture content of the stored beans affect the physicochemical and technological properties of soybeans, causing changes in antioxidant compounds and the properties of soybean protein isolate (Coradi et al., 2020; Ferreira et al., 2019; Ziegler et al., 2016).

Among the technologies used to maintain soybean quality in the postharvest phase, aeration is the most used to maintain, standardize and/or reduce the temperature of soybean grain mass during storage (Coradi et al., 2020). Grain aeration is an established low-cost, chemical-free technology to maintain favorable storage conditions for safe preservation of grain quality (Lopes & Neto, 2022).

The accurate prediction of the stored grain ecosystem is essential to develop and evaluate aeration strategies that are adapted to the climate characteristics of the storage region. Methods for predicting grain temperature and moisture can be used to evaluate the effectiveness of aeration and estimate whether chemical treatments are necessary to combat insects, mites, and fungi. However, testing various aeration strategies to establish best practices for preserving stored grain masses can be costly, as it requires monitoring temperature and moisture at multiple points in a large number of grain silos, and over multiple seasons (El Melki et al., 2022).

Mathematical models related to aeration, can be used to predict the temperature and moisture of stored grain under different climatic conditions and aeration strategies. Generally, these models are used to evaluate the effectiveness of ambient air aeration, to estimate the maximum safe storage period of grain, and to predict the aeration time required (El Melki et al., 2022). In addition, the most promising results during simulation can be tested in the field (Nuttall et al., 2017).

Several mathematical models can be found in the literature involving the aeration process, such as, Thompson et al. (1968), Sinicio et al. (1997), Canchun et al. (2001), Thorpe (2001b) and Khatchatourian & Oliveira (2006).

Rigoni et al. (2022) presented a manufactured analytical solution using the method of manufactured solutions (MMS) for the mathematical model that describes the behavior of the grain mass aeration process proposed by Thorpe (2001b), which is widely used in the literature (Lopes et al., 2006, 2014, 2015; Rigoni & Kwiatkowski Jr, 2020). The

* Corresponding author.
E-mail addresses: rigoni1@ufpr.br (D. Rigoni), marcio_villela@ufpr.br (M.A.V. Pinto), jotair@unicentro.br (J.E. Kwiatkowski Jr).

https://doi.org/10.1016/j.compag.2023.108300
Received 4 May 2023; Received in revised form 2 August 2023; Accepted 29 September 2023

Nomenclature

Abbreviations

CDS	Central difference scheme
FDM	Finite difference method
MMS	Method of manufactured solutions
PDE	Partial differential equation
TDMA	Tri Diagonal matrix algorithm

Variables

A, B, C	Constants that vary according to the type of grain
c_a	Specific heat of air $\left(Jkg^{-1^\circ}C^{-1}\right)$
c_g	Grain specific heat $\left(Jkg^{-1^\circ}C^{-1}\right)$
C_i	Coefficients
c_W	Specific heat of water $\left(Jkg^{-1^\circ}C^{-1}\right)$
D	Dimensionless constant
dm/dt	Derivative of the grain dry matter loss with respect to time (kgs^{-1})
Δt	Difference between the current simulation time and the previous one
Δy	Spacing between two consecutive nodes
E	Numerical error
ϵ	Grain porosity (decimal)
$erfc$	Complementary error function
$\mathscr{T}_1$	Auxiliary variable used in the mathematical model
$\mathscr{T}_2$	Auxiliary variable used in the mathematical model
h	Representative mesh size
h_s	Differential heat of sorption (Jkg^{-1})
h_v	Latent heat of vaporization of water (Jkg^{-1})
M_T	Parameter used to adjust the aeration time according to the temperature
M_U	Parameter used to adjust the aeration time according to the water content
N	Number of unknowns
n	Temporal location of the node
N_t	Number of time steps
N_y	Number of nodes in the y direction
P	Central node
P_1	Dummy variable used in the analytical solution
P_2	Dummy variable used in the analytical solution
P_3	Dummy variable used in the analytical solution
P_{atm}	Atmospheric pressure (Pa)
p_E	Effective order
p_L	Asymptotic order
p_U	Apparent order
p_s	Saturation vapor pressure (Pa)
q	Mesh refinement ratio
Q_r	Heat of oxidation of the grain $(Js^{-1}m^{-3})$
R	Humidity ratio of air $(kgkg^{-1})$
ρ_a	Density of intergranular air (kgm^{-3})
ρ_σ	Grain bulk density (kgm^{-3})
r_a	Relative humidity of the aeration air (%)
r_u	Equilibrium relative humidity (%)
S, $\mathscr{A}$, $\mathscr{B}$, $\mathscr{T}$	Parameters used to simplify notation
S_T	Source term
T	Grain temperature (°C)
$\widehat{T}$	Grain temperature obtained analytically (°C)
t	Time (s)
θ	Represents the temporal formulation used
T_{amb}	Ambient temperature (°C)
$T_{An}(y)$	Represent the analytically obtained temperature (°C)
T_B	Aeration air temperature (°C)
t_f	Final simulation time (s)
T_I	Initial grain temperature (°C)
U	Grain moisture $(kgkg^{-1})$
$\mathscr{U}_1$	Auxiliary variable used in the moisture numerical solution
$\mathscr{U}_2$	Auxiliary variable used in the moisture numerical solution
u_a	Aeration air velocity (ms^{-1})
U_I	Initial grain moisture $(kgkg^{-1})$
U_p	Initial grain moisture content in percent (%)
u_r	Ambient relative humidity (%)
W, E	Identifiers of the position of discrete points in relation to a central node
y	Axis in the vertical direction (oriented from bottom to top) (m)

mathematical model was solved numerically using the Finite Difference Method (FDM). In contrast to related works in the literature, several numerical approximations were used to solve the mathematical model, and the CDS-Crank-Nicolson and Leith's methods were recommended by the authors.

Alauzet & Loseille (2016) reported that in some physical phenomena, uniform meshes are not ideal. These phenomena are anisotropic in nature. Thus, it seems natural to take into account the properties of physical phenomena within the mesh in order to improve its representation. Still, there is no study in the literature on geometrical anisotropic factors, referred to in this paper as space–time ratios, in the numerical solution of the mathematical model proposed by Thorpe (2001b).

The purpose of this paper is to solve the mathematical model proposed by Thorpe (2001b) by means of the FDM and to conduct a study on the performance of the CDS-Crank-Nicolson and Leith's methods when employing a variety of space–time ratios, that represents the anisotropic factors, in two different settings of soybeans aeration. Furthermore, this paper compares the results with an adaptation of the manufactured analytical solution, proposed by Rigoni et al. (2022), that takes into account more realistic parameters.

This work also includes performing an analysis of the discretization error for the approximations used. As in Rigoni et al. (2022), Xuan et al. (2017), Mousa & Ma (2020) and Melland et al. (2021), the technique presented by Von Neumann & Richtmyer (1950) was chosen to treat the non-physical oscillations in the second-order approximations.

The remainder of this paper is organized as follows. In section 2, the mathematical model proposed by Thorpe (2001b), the boundary and initial conditions are presented. In section 3, an adaptation of the manufactured analytical solution proposed in Rigoni et al. (2022) is introduced in order to contemplate more realistic parameters. The numerical model is detailed in section 4. In section 5, the numerical verification of the code is performed, and the computational details are exposed. In section 6, the results obtained are presented and discussed, and in section 7, the conclusions are drawn.

2. Mathematical model

The model that describes the temperature (T) and grain moisture (U) used in this work was presented in detail by Thorpe (2001b) and according to Lopes et al. (2006) the model relates air psychometric relationships with mass and energy balances. Additionally, according to Lopes et al. (2006), some simplifications can be made to the original model without loss of accuracy. The simplified model, adopted in this work, is given by

$$\frac{\partial T}{\partial t}\left(\rho_\sigma\left[c_g + c_W U\right] + \epsilon\rho_a\left[c_a + R\left(c_W + \frac{\partial h_v}{\partial T}\right)\right]\right) =$$

$$\rho_\sigma h_s \frac{\partial U}{\partial t} - u_a \rho_a \left[c_a + R\left(c_W + \frac{\partial h_v}{\partial T} \right) \right] \frac{\partial T}{\partial y} + \rho_\sigma \frac{dm}{dt}(Q_r - 0.6 h_v), \quad (1)$$

$$\rho_\sigma \frac{\partial U}{\partial t} = -u_a \rho_a \frac{\partial R}{\partial y} + \frac{dm}{dt}(0.6 + U), \quad (2)$$

where: t is time (s), y is the axis in the vertical direction (oriented from bottom to top) (m), U is grain moisture ($kgkg^{-1}$), u_a is aeration air velocity (ms^{-1}), c_g is grain specific heat $\left(Jkg^{-1^\circ}C^{-1}\right)$,$c_W$ is specific heat of water $\left(Jkg^{-1^\circ}C^{-1}\right)$, c_a is specific heat of air $\left(Jkg^{-1^\circ}C^{-1}\right)$, R is humidity ratio of air ($kgkg^{-1}$), ρ_a is density of intergranular air (kgm^{-3}), ρ_σ is grain bulk density (kgm^{-3}), h_v is latent heat of vaporization of water (Jkg^{-1}), h_s is differential heat of sorption (Jkg^{-1}), T is grain temperature (°C), ϵ is grain porosity (decimal), dm/dt is derivative of the grain dry matter loss with respect to time (kgs^{-1}) and Q_r is heat of oxidation of the grain ($Js^{-1}m^{-3}$).

An aeration system with up flow, that is, $y \in [0, L]$, was considered, where L represents the height of the grain mass, as shown in Fig. 1. Therefore, a one-dimensional simplification of the model was considered. Although this paper handles a one-dimensional simplification, Fig. 1 shows a realistic three-dimensional silo for a better visualization of the problem geometry.

The aeration air velocity (u_a) is the velocity at which air flows through the stored grain mass. According to Brooker et al. (1992), the specific heat of water (c_W) and the specific heat of air (c_a) are well-defined quantities, equals to 4186 $\left(Jkg^{-1^\circ}C^{-1}\right)$ and 1000 $\left(Jkg^{-1^\circ}C^{-1}\right)$, respectively.

The porosity of soybeans (ϵ) is the ratio between the volume occupied by air in the grain mass and the total volume occupied by that mass. Such porosity considerably influences the pressure of air flows passing through the grain mass. In this study it was used $\epsilon = 0.361$, obtained by Brooker et al. (1992).

The density of the grain mass (ρ_σ) determines the volume required to store a given amount of a product and directly influences the airflow rate required for aeration and the heat and mass transfer process in the storage environment (Lopes et al., 2006). The density value of the soybean grain mass ($\rho_\sigma = 737kgm^{-3}$) was considered based on the data shown by Thorpe (2001a).

According to Fleurat-Lessard (2002), the heat of oxidation of the grain (Q_r) is equal to 15,778 ($Js^{-1}m^{-3}$). The specific heat of grain (c_g) also affects the heat and mass transfer process during aeration (Navarro & Noyes, 2001), and as stated by Lopes et al. (2006), it represents the amount of heat energy required to increase the temperature of 1 kg of a product by 1 °C. Data from Jayas & Cenkowski (2006) were used to determine the specific heat of soybean $\left(c_g = 1637Jkg^{-1^\circ}C^{-1}\right)$.

The differential heat of sorption (h_s), as well as the latent heat of vaporization of water (h_v), are essential properties considered in the simulation of the aeration process, as they interfere in the heat and mass transfer within the storage environment (Lopes et al., 2006). According to Thorpe (2001b), h_s is the total energy required to remove one unit mass of water from the grain mass and is given by

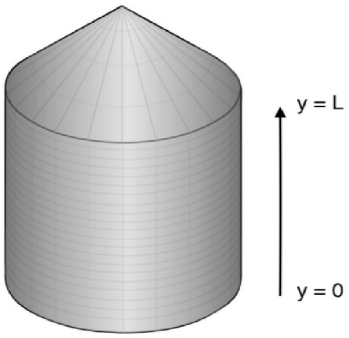

Fig. 1. Calculation Domain.

$$h_s = h_v \left[1 + \frac{Ae^{-BU}(T + 273.15)}{(T + C)^2 - 5 + \frac{6800}{T + 273.15}} \right], \quad (3)$$

where A, B, and C are constants that vary according to grain type, as detailed by Pfost et al. (1976).

As mentioned by Thorpe (2001b), the heat applied to water that turns it from liquid to vapor is called the latent heat of vaporization of water (h_v) and can be calculated by

$$h_v = 2501.33 - 2.363T. \quad (4)$$

In order to correct for possible altitude effects, the intergranular air density (ρ_a) can be calculated, as (Lopes et al., 2006):

$$\rho_a = \frac{258.8 P_{atm}}{101.325(T + 273.15)}, \quad (5)$$

where P_{atm} is the atmospheric pressure.

With respect to time, the derivative of the dry matter loss of the grain (dm/dt) can be estimated through models obtained by fitting mathematical relationships to experimental data. In this paper, the model presented by Thompson (1972) was adopted:

$$\frac{dm}{dt} = 8.83 \times 10^{-4} \left\{ exp\left[1.667 \times 10^{-6} \frac{t}{M_U M_T} \right] - 1 \right\} + 2.833 \times 10^{-9} \frac{t}{M_U M_T}, \quad (6)$$

where M_U and M_T are parameters used to adjust the aeration time according to the water content and temperature of the grains. The parameter M_U can be obtained by

$$M_U = 0.103 \left\{ exp\left[\frac{455}{(100U)^{1.53}} \right] - 0.845U + 1.558 \right\}, \quad (7)$$

and M_T can be obtained depending on the temperature and moisture range:

$$M_T = S, \text{if } T \leq 15 \text{ or } U \leq 19, \quad (8a)$$

$$M_T = S + \frac{\frac{100U}{U+1} - 19}{100} exp[0.0183T - 0.2847], \text{if } T > 15 \text{ and } 19 < U < 28, \quad (8b)$$

$$M_T = S + 0.09 exp[0.0183T - 0.2847], \text{ if } T > 15 \text{ and } U \geq 28, \quad (8c)$$

and $S = 32.2exp(-0.1044T - 1.856)$.

The air humidity ratio (R) is the ratio between the mass of water vapor and the mass of dry air in a given volume of mixture. This parameter is used to model the behavior of the grain mass during the aeration process, helping to estimate the water content of the stored product and helping to predict the effects of aeration on the storage environment. This parameter can be calculated by (Thorpe, 2001a):

$$R = 0.622 \frac{r_u p_s}{P_{atm} - r_u p_s}, \quad (9)$$

where p_s is the saturation vapor pressure given as (Hunter, 1987):

$$p_s = \frac{6 \times 10^{25}}{(T + 273.15)^5} exp\left[-\frac{6800}{T + 273.15} \right], \quad (10)$$

and r_u represents the equilibrium relative humidity and can be calculated as (Chung & Pfost, 1967):

$$r_u = 100 exp\left[-\frac{A}{T + C} exp(-BU) \right]. \quad (11)$$

2.1. Boundary conditions

At $y = 0$, it was assumed that the grain at the base of the storage reaches equilibrium with the aeration airflow:

$$T(0,t) = T_B, \tag{12}$$

where T_B represents the aeration air temperature.

The moisture content at $y = 0$ was calculated as:

$$U(0,t) = -\frac{1}{B} ln\left[ln\left(-\frac{r_a}{100}\right)\left(-\frac{T_B + C}{A}\right)\right] = U_B, \tag{13}$$

which is an adaptation of the Chung-Pfost equation (Eq. (11)) where r_a represents the relative humidity of the aeration airflow and can be obtained by

$$r_a = u_r \frac{\frac{6\times10^{25}}{(T_{amb}+273.15)^5} exp\left[-\frac{6800}{T_{amb}+273.15}\right]}{\frac{6\times10^{25}}{(T_B+273.15)^5} exp\left[-\frac{6800}{T_B+273.15}\right]}, \tag{14}$$

where u_r is the ambient relative humidity and T_{amb} is the ambient temperature.

At $y = L$, the Neumann boundary conditions for temperature and moisture are given by

$$\left(\frac{\partial T}{\partial y}\right)_{y=L} = \left(\frac{\partial U}{\partial y}\right)_{y=L} = 0. \tag{15}$$

2.2. Initial conditions

Throughout the domain, the initial condition is equal to the temperature of the grain mass after the drying process (T_I).

$$T(y,0) = T_I. \tag{16}$$

The initial moisture (U_I) can be obtained by (Thorpe, 2001b)

$$U(y,0) = \frac{U_p}{100 - U_p} = U_I, \tag{17}$$

where U_p is the moisture content of the grain after drying, in percent (%).

3. Proposed analytical solution

The Method of Manufactured Solutions (MMS) (Oberkampf & Blottner, 1998) consists in producing an exact solution, without any interest in the physical reality of the problem. An analytic function is defined as the dependent variable in the partial differential equation (PDE), and all derivatives are calculated analytically. The remaining terms that do not satisfy the PDE are then incorporated into a source term in the equation, which is added to the PDE to exactly satisfy the new PDE (Roy, 2005).

Despite the many uses of the model proposed by Thorpe (2001b) found in the literature, hereinafter referred to as Thorpe model, there is no investigation of the analytical solution of the mathematical model. Rigoni et al. (2022) were pioneers in proposing a manufactured analytical solution to the model proposed by Thorpe (2001b).

The manufactured analytical solution was proposed using the MMS based on experimental data presented by Khatchatourian & Oliveira (2006) and Oliveira et al. (2007). The experiment monitored the temperature of soybeans in a one-meter prototype silo ($L = 1\ m$), with thermocouples placed at heights of 0.15 m, 0.27 m, 0.40 m, and 0.54 m, during one hour of aeration with the aeration air velocity $u_a = 0.23\ m/s$. The initial grain temperature was $T_I = 52.9$ °C, and the aeration air temperature was $T_B = 31.1$ °C. The soybeans with an average water content of 12 % were previously selected and cleaned for the realization of the experiment.

The analytical solution for the Eq. (1) proposed by Rigoni et al. (2022) was manufactured based on modifying a solution of a problem presented by Van Genuchten et al. (1982), and it is given by

$$\widehat{\mathrm{T}}(\mathrm{y},\mathrm{t}) = \mathrm{T_I} + \frac{1}{2}(\mathrm{T_B} - \mathrm{T_I})\left[erfc\left(\frac{\mathrm{y} - 2.2\times10^{-4}\mathrm{t}}{\sqrt{8\times10^{-6}\mathrm{t}}}\right) + \exp\left(\frac{2.2\times10^{-4}\mathrm{y}}{8\times10^{-6}}\right) erfc\left(\frac{\mathrm{y} + 2.2\times10^{-4}\mathrm{t}}{\sqrt{8\times10^{-6}\mathrm{t}}}\right)\right], \tag{18}$$

where *erfc* represents the complementary error function (Van Genuchten et al., 1982), defined by $erfc(x) = \frac{2}{\sqrt{\pi}}\int_x^\infty e^{-t^2} dt$.

Interestingly, the solution takes as parameters the size of the storage location (y), the aeration time (t), the temperature of the aeration airflow (T_B), and the grain mass initial temperature (T_I). Although the manufactured analytical solution proposed by Rigoni et al. (2022) showed excellent results when compared to experimental data, it did not consider aeration air velocity (u_a) as an initial parameter. To address this, algebraic manipulations were performed in the solution and a new manufactured analytical solution that accounts this parameter was proposed. Thus, the new manufactured analytical solution, proposed in this paper, is given by:

$$\widehat{T}(y,t) = T_I + \frac{1}{2}(T_B - T_I)[erfc(P_1) + exp(P_2)erfc(P_3)], \tag{19}$$

$$P_1 = \frac{y - u_a\frac{2.2\times10^{-4}}{0.23}t}{\sqrt{u_a\frac{8\times10^{-6}}{0.23}t}},\quad P_2 = \frac{u_a\frac{2.2\times10^{-4}}{0.23}y}{u_a\frac{8\times10^{-6}}{0.23}} \quad \text{and} \quad P_3 = \frac{y + u_a\frac{2.2\times10^{-4}}{0.23}t}{\sqrt{u_a\frac{8\times10^{-6}}{0.23}t}}$$

Fig. 2 shows Eq. (19) applied to the same points as the experimental data (Khatchatourian & Oliveira, 2006; Oliveira et al., 2007), using $y = 1\mathrm{m}, t = 3600s, T_I = 52.9$ °C, $T_B = 31.1$ °C and $u_a = 0.23m/s$.

The comparison between the manufactured analytical solution (depicted in red) and the experimental data (displayed in blue) reveals striking similarities in their behavior.

Additionally, intriguing patterns emerge when examining the grain temperature decline in different layers. For instance, a noticeable drop occurs at approximately 450 s for the layer at y = 0.15 m, around 1,000 s for the layer at y = 0.27 m, roughly 1,500 s for the layer at y = 0.40 m, and approximately 2,000 s for the layer at y = 0.54 m. Furthermore, as the grain temperature stabilizes, distinct time intervals are observed, such as after 1,250 s for the layer at y = 0.15 m, about 2,000 s for the layer at y = 0.27 m, approximately 2,750 s for the layer at y = 0.40 m, and around 3,550 s for the layer at y = 0.54 m. Remarkably, throughout these phases, the manufactured analytical solution, developed in this study, exhibits a high level of concurrence with the experimental data.

The manufactured analytical solution proposed in this paper, given

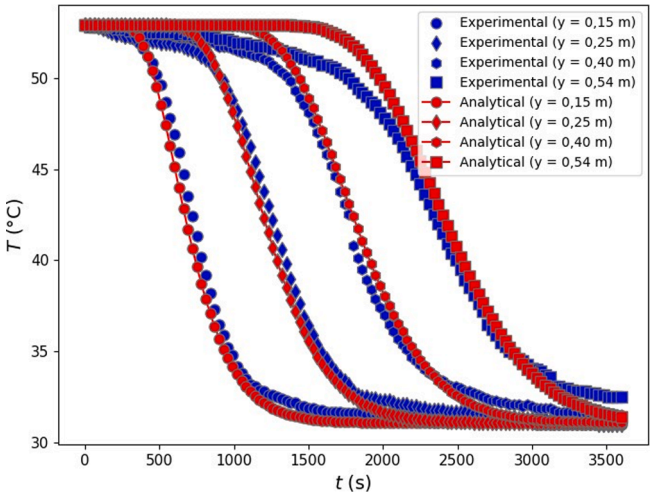

Fig. 2. Manufactured analytical solution and the experimental data (Rigoni et. al, 2022; Khatchatourian & Oliveira, 2006; Oliveira et al., 2007).

by Eq. (19), satisfies the conditions of real aeration systems, which can take between 300 and 600 h to complete, have different geometries, different grain initial temperatures, different airflow temperatures, and different aeration air temperature with minor modifications. Regarding different initial moisture, more elaborate modifications are required, and such adaptations should be further investigated.

For the function defined by Eq. (19) to be considered a manufactured analytical solution, a source term (S_T) must be added to Eq. (1), thus:

$$\frac{\partial T}{\partial t}\left(\rho_\sigma\left[c_g + c_W U\right] + \epsilon\rho_a\left[c_a + R\left(c_W + \frac{\partial h_v}{\partial T}\right)\right]\right) =$$

$$\rho_\sigma h_s \frac{\partial U}{\partial t} - u_a\rho_a\left[c_a + R\left(c_W + \frac{\partial h_v}{\partial T}\right)\right]\frac{\partial T}{\partial y} + \rho_\sigma \frac{dm}{dt}(Q_r - 0.6h_v) + S_T, \tag{20}$$

where S_T is given by

$$S_T = \frac{\partial \widehat{T}}{\partial t}\left(\rho_\sigma\left[c_g + c_W U\right] + \epsilon\rho_a\left[c_a + R\left(c_W + \frac{\partial h_v}{\partial T}\right)\right]\right)$$

$$-\rho_\sigma h_s \frac{\partial U}{\partial t} + u_a\rho_a\left[c_a + R\left(c_W + \frac{\partial h_v}{\partial T}\right)\right]\frac{\partial \widehat{T}}{\partial y} - \rho_\sigma \frac{dm}{dt}(Q_r - 0.6h_v). \tag{21}$$

In addition, $\frac{\partial \widehat{T}}{\partial t}$ and $\frac{\partial \widehat{T}}{\partial y}$ must be calculated. Substituting Eq. (21) into Eq. (20), making some simplifications and denoting $\mathscr{A}$, $\mathscr{B}$ and $\mathscr{F}$ as

$$\mathscr{A} = \rho_\sigma\left[c_g + c_W U\right] + \epsilon\rho_a\left[c_a + R\left(c_W + \frac{\partial h_v}{\partial T}\right)\right], \tag{22}$$

$$\mathscr{B} = u_a\rho_a\left[c_a + R\left(c_W + \frac{\partial h_v}{\partial T}\right)\right], \tag{23}$$

$$\mathscr{F} = \mathscr{A}\left(\frac{\mathscr{F}_1}{2}(T_B - T_I)\right) + \mathscr{B}\left(\frac{\mathscr{F}_2}{2}(T_B - T_I)\right), \tag{24}$$

where,

$$\mathscr{F}_1 = \frac{1}{(tu_a)^{\frac{3}{2}}}0.0457519u_a(T_B - T_I)exp\left(-\frac{28.750y^2}{tu_a} - 0.0263043tu_a - 27.5y\right)\{y[1045.45 + 1045.45exp(82.5y)] + + tu_a(exp(82.5y) - 1)\}$$

$$\mathscr{F}_2 = 27.5exp(27.5y)erfc\left(\frac{169.558(0.000956522tu_a + y)}{\sqrt{tu_a}}\right) + \frac{1}{\sqrt{tu_a}}\left(-191.326exp\left(-\frac{28.75y^2}{tu_a}\right) + -0.026043tu_a - 27.5y\right) - 191.326exp\left[-\left(\frac{28750(y - 0.000956522tu_a)^2}{tu_a}\right)\right]$$

the equation that describes the temperature (T) of the grain mass is presented as follows:

$$\mathscr{A}\frac{\partial T}{\partial t} = -\mathscr{B}\frac{\partial T}{\partial y} + \mathscr{F}, \tag{25}$$

which its analytic solution is given by Eq. (19) through MMS.

Remark. This study addresses the resolution of the temperature problem in soybeans during the aeration process using the method of manufactured solutions. The proposed approach involves creating a specific analytical solution for the grain temperature, as the experiment used as basis only measured the grain temperature.

By employing the method of manufactured solutions, a known analytical solution can be developed for the particular problem without the need to address all physical properties of the system. It is important to note that although the developed analytical solution in this study does not include terms related to grain moisture, it does not diminish the practical utility of the approach. In this study, the exclusive analytical solution for soybean grain temperature provides a strategic approach to assess the accuracy and efficiency of the numerical approximations utilized to resolve the soybean grain temperature model during the aeration process. The focus is on understanding the behavior of temperature and evaluating the performance of numerical approximations concerning this specific variable.

Furthermore, this methodology facilitates the identification and quantification of the space–time ratio effects in the obtained solutions, providing valuable insights into the quality of the numerical results and the necessity for potential adjustments or improvements in the adopted approximations.

The mathematical model used in this study was proposed by Thorpe (2001b), encompassing both the mass balance equation and the energy balance equation. Hence, the study accounts for the key physical factors involved in the aeration process of soybeans, despite the emphasis on temperature. This methodology offers insights into the quality of the numerical results and contributes to enhancing the understanding of this complex phenomenon.

4. Numerical model

The differential equations that describe grain temperature and moisture were solved numerically using the Finite Difference Method (FDM) (Tannehill et al., 1997). Once a given equation is discretized using this method, the evaluation of the variables and the approximations of their derivatives at the mesh nodes give rise to a system of equations that must be solved by an appropriate method, commonly called solver. In this study, a solver widely adopted in the literature called TriDiagonal Matrix Algorithm (TDMA) (Thomas, 1949) was used. For more complex systems, multigrid methods are among the most efficient techniques for solving large systems of equations arising from the discretization of PDEs and can achieve convergence rates independent of the problem size (Oliveira et al., 2018).

W and E were used to identify the position of discrete points with respect to a central node P, and n indicates the temporal location of the node, as shown in Fig. 3. In the same figure, $\Delta y = L/N_y$ corresponds to the spacing between two consecutive nodes, where N_y is the number of nodes in the y direction; and $\Delta t = t_f/N_t$, the difference between the current and the previous simulation time. Here, t_f is the final simulation time and N_t corresponds to the number of time steps.

4.1. Central difference scheme (CDS)

Approximating the spatial derivative of T using CDS and the temporal derivative of T using the θ-formulation (Tannehill et al., 1997), the discretized form of Eq. (25) is given by:

$$\mathscr{A}^\theta T_P^{n+1} = \mathscr{A}^\theta T_P^n - \frac{\mathscr{B}^\theta}{2}\left(\frac{\Delta t}{\Delta y}\right)T_E^\theta + \frac{\mathscr{B}^\theta}{2}\left(\frac{\Delta t}{\Delta y}\right)T_W^\theta + \mathscr{F}\Delta t, \tag{26}$$

where

$$\mathscr{A}^\theta = \rho_\sigma\left[c_g + c_W U_P^\theta\right] + \epsilon\rho_a\left[c_a + R_P^\theta\left(c_W + \frac{\partial h_v}{\partial T}\right)\right], \tag{27}$$

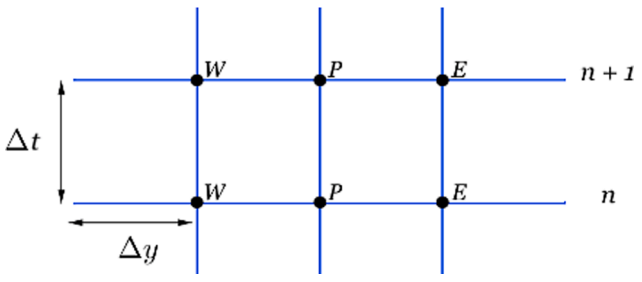

Fig. 3. Mesh of the numerical solution using FDM, for a central node P and its spatial and temporal neighbors.

$$\mathscr{B}^{\theta} = u_a\rho_a\left[c_a + R_P^{\theta}\left(c_W + \frac{\partial h_v}{\partial T}\right)\right]. \tag{28}$$

Using the same approximations for U and R, the discretized form of Eq. (2) is obtained:

$$U_P^{n+1} = U_P^n - \frac{u_a\rho_a}{2\rho_\sigma}\left(\frac{\Delta t}{\Delta y}\right)R_E^{\theta} + \frac{u_a\rho_a}{2\rho_\sigma}\left(\frac{\Delta t}{\Delta y}\right)R_W^{\theta} + \frac{\Delta t\frac{dm}{dt}}{\rho_\sigma}U_P^{\theta} + 0.6\frac{\Delta t\frac{dm}{dt}}{\rho_\sigma}, \tag{29}$$

in which the relation for an arbitrary variable Λ is given by

$$\Lambda^{\theta} = \Lambda^n + \theta\left(\Lambda^{n+1} - \Lambda^n\right), \tag{30}$$

where the Crank-Nicolson formulation is obtained for θ = 0.5 (Tannehill et al., 1997).

The Neumann boundary conditions can be approximated using CDS with the ghost point technique (Tannehill et al., 1997), so the temperature T and the moisture U at $y = L$ can be calculated, respectively, by

$$T_{N_B}^{n+1} = T_{N_B}^n + \mathscr{F}\frac{\Delta t}{\mathscr{A}}, \tag{31}$$

$$U_{N_B}^{n+1} = U_{N_B}^n + \frac{\Delta t\frac{dm}{dt}}{\rho_\sigma}U_P^{\theta} + 0.6\frac{\Delta t\frac{dm}{dt}}{\rho_\sigma}, \tag{32}$$

where N_B represents the node located at the boundary, as shown in Fig. 4.

4.2. Leith's scheme

Equation (25) can be rewritten as

$$\frac{\partial T}{\partial t} = -\left(\frac{\mathscr{B}}{\mathscr{A}}\right)\frac{\partial T}{\partial y} + \frac{\mathscr{F}}{\mathscr{A}}. \tag{33}$$

Leith's scheme (Leith, 1965) consists in approximating the temporal and spatial derivatives of a given variable, in this case T, as follows:

$$\left(\frac{\partial T}{\partial t}\right)_P^{n+1} \approx \left[\frac{T_P^{n+1} - T_P^n}{\Delta t}\right], \tag{34}$$

$$\left(\frac{\partial T}{\partial y}\right)_P^{n+1} \approx \left(\frac{\mathscr{B}}{\mathscr{A}}\right)\left(\frac{\Delta t}{\Delta y}\right)\left[\frac{T_P^n - T_W^n}{\Delta y}\right] + \left[1 - \left(\frac{\mathscr{B}}{\mathscr{A}}\right)\left(\frac{\Delta t}{\Delta y}\right)\right]\left[\frac{T_E^n - T_W^n}{2\Delta y}\right]. \tag{35}$$

Thus, the discretized form of Eq. (33) is achieved:

$$\begin{aligned} T_P^{n+1} = {} & \left[1 - \left(\frac{\mathscr{B}}{\mathscr{A}}\frac{\Delta t}{\Delta y}\right)^2\right]T_P^n + \frac{1}{2}\left[\left(\frac{\mathscr{B}}{\mathscr{A}}\frac{\Delta t}{\Delta y}\right)^2 + \left(\frac{\mathscr{B}}{\mathscr{A}}\frac{\Delta t}{\Delta y}\right)\right]T_W^n \\ & + \frac{1}{2}\left[\left(\frac{\mathscr{B}}{\mathscr{A}}\frac{\Delta t}{\Delta y}\right)^2 - \left(\frac{\mathscr{B}}{\mathscr{A}}\frac{\Delta t}{\Delta y}\right)\right]T_E^n + \mathscr{F}\frac{\Delta t}{\mathscr{A}}. \end{aligned} \tag{36}$$

The same procedure can be done in Eq. (2), resulting in the discretized form, given by

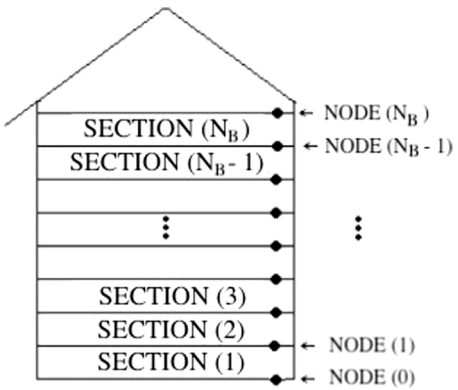

Fig. 4. Discretized domain.

$$U_P^{n+1} = \left[\frac{2\rho_\sigma}{2\rho_\sigma - \frac{dm}{dt}\Delta t}\right](\mathscr{U}_1 + \mathscr{U}_2), \tag{37}$$

where

$$\mathscr{U}_1 = \left(1 + \frac{\frac{dm}{dt}\Delta t}{2\rho_\sigma}\right)U_P^n - \left(\frac{u_a\rho_a}{\rho_\sigma}\frac{\Delta t}{\Delta y}\right)^2 R_P^n + \frac{1}{2}\left[\left(\frac{u_a\rho_a}{\rho_\sigma}\frac{\Delta t}{\Delta y}\right)^2 + \left(\frac{u_a\rho_a}{\rho_\sigma}\frac{\Delta t}{\Delta y}\right)\right]R_W^n$$

$$\mathscr{U}_2 = +\frac{1}{2}\left[\left(\frac{u_a\rho_a}{\rho_\sigma}\frac{\Delta t}{\Delta y}\right)^2 - \left(\frac{u_a\rho_a}{\rho_\sigma}\frac{\Delta t}{\Delta y}\right)\right]R_E^n + \frac{0.6\Delta t\frac{dm}{dt}}{\rho_\sigma}.$$

Neumann boundary conditions can be approximated using the ghost point technique (Tannehill et al., 1997), whose results are analogous to Eqs. (31) and (32).

4.3. Artificial viscosity

Originally introduced by Von Neumann & Richtmyer (1950), the artificial viscosity is a method to control spurious non-physical oscillations in numerical solutions and can be added to the temperature equation. Thus, Eq. (25) can be rewritten as

$$\mathscr{A}\frac{\partial T}{\partial t} = -\mathscr{B}\frac{\partial T}{\partial y} + \frac{\partial}{\partial y}\left[D\Delta y^2\left|\frac{\partial T}{\partial y}\right|\frac{\partial T}{\partial y}\right] + \mathscr{F}, \tag{38}$$

where D is a dimensionless constant (Campbell & Vignjevic, 2009). Note that, as $\Delta y \to 0$, the term corresponding to the artificial viscosity tends to zero. Therefore, Eq. (38) tends to Eq. (25).

The method presented by Lax & Wendroff (1960) was used to perform the discretization. For the problem in this study, the artificial viscosity was used to eliminate excessive oscillations in the second-order methods. In this regard, it is appropriate to add the following term in the discretized equations of these methods:

$$\frac{\partial}{\partial y}\left[D\Delta y^2\left|\frac{\partial T}{\partial y}\right|\frac{\partial T}{\partial y}\right] \approx \frac{D}{\Delta y}\left[\left|T_E^n - T_P^n\right|\left(T_E^n - T_P^n\right) - \left|T_P^n - T_W^n\right|\left(T_P^n - T_W^n\right)\right]. \tag{39}$$

With the purpose of providing a comprehensive understanding and facilitating the replication of this work, the computational implementation algorithm of the Thorpe model for grain aeration is presented here. It utilizes the finite difference method with the Leith approximation.

Algorithm: Temperature and moisture calculation – Leith's scheme.

- Entry:$u_a, c_W, c_a, Q_r, \epsilon, \rho_\sigma, c_g, A, B, C, u_r, u_i, P_{atm}, T_B, T_I, L, t_f, N_y, N_t$
- Calculate the values of Δy and Δt
- Initialize:$T(1:N_y, 1:N_t), U(1:N_y, 1:N_t), R(1:N_y, 1:N_t)$
- **For** $(n = 1)$ and $(i = 1:N_y)$ **do**
- $T(i,1) = T_I$[Eq. (16)]
- $U(i,1) = U_I$[Eq. (17)]
- **End for**
- **For** $(i = 1:N_y)$ and $(n = 1)$ **do**
- Calculate the saturation vapor pressure p_s [Eq. (10)]
- Calculate the equilibrium relative humidity r_u [Eq. (11)]
- Calculate the initial mixing ratio $R(i,1)$ [Eq. (9)]
- **End for**
- **For** $(n = 2:N_t)$ and $(i = 1:N_y)$ **do**
- **If** $(i = 1)$ **then**
  - Calculate the density of air ρ_a [Eq. (5)]
  - Calculate the relative humidity of the aeration air r_a [Eq. (14)]
  - The saturation vapor pressure is calculated (using r_a) ρ_{sa} [Eq. (10)]
  - The mixing ratio at $y = 0(R(1,n))$ is calculated [Eq. (9)]
  - The moisture at $y = 0(U(1,n))$ is calculated [Eq. (13)]
  - The temperature at y = 0 (T(1, n)) is calculated [Eq. (12)]
- **End if**
- **If** $(i = 2:N_y - 1)$ **then**
  - The loss of dry matter in relation to time is calculated dm/dt [Eq. (6)]

(continued on next page)

(*continued*)

Algorithm: Temperature and moisture calculation – Leith's scheme.

- The saturation vapor pressure is calculated ρ_s [Eq. (10)]
- The equilibrium relative humidity pressure is calculated r_u [Eq. (11)]
- Calculate the mixing ratio $R(i,n)$ [Eq. (9)]
- The moisture $U(i,n)$ is calculated [Eq. (37)]
- The loss of dry matter in relation to time is calculated dm/dt [Eq. (6)]
- The specific enthalpy of vaporization of water is calculated h_v [* Derivative of Eq. (4)]
- Calculate the derivative of the enthalpy of vaporization of water with respect to temperature $\frac{\partial h_v}{\partial T}$ [Eq. (4)]
- Calculate differential enthalpy of sorption h_s [Eq. (3)]
- The temperature $T(i,n)$ is calculated [Eq. (36)]

o **End if**

o **If** $(i = 2 : N_y - 1)$ **then**

- The saturation vapor pressure in $y = L$ is calculated ρ_s [Eq. (10)]
- The equilibrium relative humidity pressure in $y = L$ is calculated r_u [Eq. (11)]
- Calculate the mixing ratio $R(N_y,n)$ [Eq. (9)]
- The moisture $U(N_y,n)$ is calculated [Eq. (32)]
- The loss of dry matter in relation to time in $y = L$ is calculated dm/dt [Eq. (6)]
- The specific enthalpy of vaporization of water in $y = L$ is calculated h_v [Eq. (4)]
- Calculate the derivative of the enthalpy of vaporization of water with respect to temperature in $y = L$ [* Derivative of Eq. (4)]
- Calculate differential enthalpy of sorption in $y = L$ h_s [Eq. (3)]
- The temperature $T(N_y,n)$ is calculated [Eq. (31)]

o **End if**

o **End for**

5. Numerical verification results

In this section, a comprehensive analysis of the code to ensure accuracy and reliability of our results is provided. The section is divided into four parts: error analysis, computational details, manufactured analytical solution, and numerical verification.

5.1. Error analysis

Given that a new manufactured analytical solution was proposed in this paper, it is essential to elaborate an error analysis similar to the one performed by Rigoni et al. (2022). According to Marchi et al. (2016), the numerical error E(ϕ) on a given variable of interest is defined as the difference between the exact analytical solution Φ and the numerical solution ϕ:

$$E(\phi) = \Phi - \phi, \tag{40}$$

where $E(\phi)$ can appear in four forms (Marchi et al., 2016): truncation, iteration, rounding and programming. When the other sources can be neglected, the truncation error (here called discretization error) $E(\phi)$ is given, according to Roache (1998), by

$$E(\phi) = C_1 h^{p_1} + C_2 h^{p_2} + C_3 h^{p_3} + \cdots, \tag{41}$$

where h is the representative mesh size, $C_i, i = 1, 2, 3, \ldots$, are coefficients that are independent of h, but depend on the variable in question, and p_i, with $p_1 < p_2 < p_3 < \ldots$, are positive integers called true orders of the error. The first true order is called the asymptotic order and is denoted by $p_L = p_1$. The asymptotic order is a theoretical result obtained from the types of approximations used to discretize the problem.

The developed numerical model can be used to verify if the asymptotic order of the discretization error is achieved. If the analytical solution to the problem is available, the effective order p_E of the discretization error can be used to estimate the asymptotic order. If the analytical solution is unknown, the apparent order p_U can be used to estimate the asymptotic order. The effective and apparent orders can be calculated, respectively, by (Marchi et al., 2016)

$$p_E = \frac{log\left(\frac{\Phi-\phi_2}{\Phi-\phi_1}\right)}{log(q)}, \tag{42}$$

$$p_U = \frac{log\left(\frac{\phi_2-\phi_3}{\phi_1-\phi_2}\right)}{log(q)}, \tag{43}$$

where ϕ_1, ϕ_2, ϕ_3, h_1, h_2 and h_3 are the numerical solutions and the representative sizes of the fine, coarse, and super coarse meshes, respectively, and $q = h_2/h_1 = h_3/h_2$ is the mesh refinement ratio. Theoretically, the effective and apparent orders tend to the asymptotic order with mesh refinement, $p_E \to p_L$ and $p_U \to p_L$ when $h \to 0$ (Marchi et al., 2016). Table 1 shows the asymptotic order of each method used (Dehghan, 2005; Campbell & Yin, 2007; Tannehill et al., 1997).

5.2. Computational details

The numerical resolutions were obtained using codes written in Fortran 95, using Microsoft Visual Studio Code v. 1.62.0 with quadruple precision, and were compiled on a computer with a 3.4 GHz Intel Core i5 Quad-Core processor with 8 GB of DDR3 RAM and a 2 GB AMD Radeon 7850 graphics card.

Simulations were performed varying the space–time ratio between the spatial and temporal meshes, $\lambda = N_t/N_y$, for each method used, CDS-Crank-Nicolson and Leith. This space–time ratio represents the distortion between the spatial and temporal meshes. In this paper $\lambda = 2, 4, 8,$ 16 and 32 were used.

Two different settings of the soybean aeration process were simulated, taking into consideration important information reported by Jayas & Muir (2001), which presents a series of parameters related to the power/speed ratio of the aeration fans for different sizes of storage locations. Such settings will be detailed in section 6 of numerical experiments.

5.3. Manufactured analytical solution

Fig. 5 illustrates the manufactured analytical solution of the temperature, as given by Eq. (19), for four different variations of the aeration air velocity ($u_a = 0.05$, 0.15, 0.23, and 0.5), using the experimental parameters made by Khatchatourian & Oliveira (2006) and Oliveira et al. (2007) ($T_I = 52.9$ °C, $T_B = 31.1$ °C and L = 1 m). The figure shows the temperature profile as a function of distance (L, given in meters) and time (given in hours).

It can be observed from Fig. 5 that the new manufactured analytical solution exhibits an interesting behavior with changes in the aeration air velocity. Specifically, in Fig. 5.1, it is evident that only the grains located near the base of the storage location suffered cooling at the end of one hour of aeration. Similarly, in Fig. 5.2, it can be observed that the grains located in the lower half of the storage location suffered cooling after one hour of aeration.

In Fig. 5.3, where $u_a = 0.23$ was used, the same velocity as in Rigoni et al. (2022), the solutions show identical performance. This associativity suggests that the solution proposed in this work exhibits similar behavior to the experimental data. In addition, when the aeration air velocity is considerably high, as shown in Fig. 5.4, the grain mass rapidly approaches the aeration air temperature.

The new manufactured analytical solution, proposed in this work,

Table 1
Asymptotic order of each method used (Dehghan, 2005; Campbell & Yin, 2007; Tannehill et al., 1997).

Method	Asymptotic Order (p_L)
CDS-Crank-Nicolson	2
Leith	2

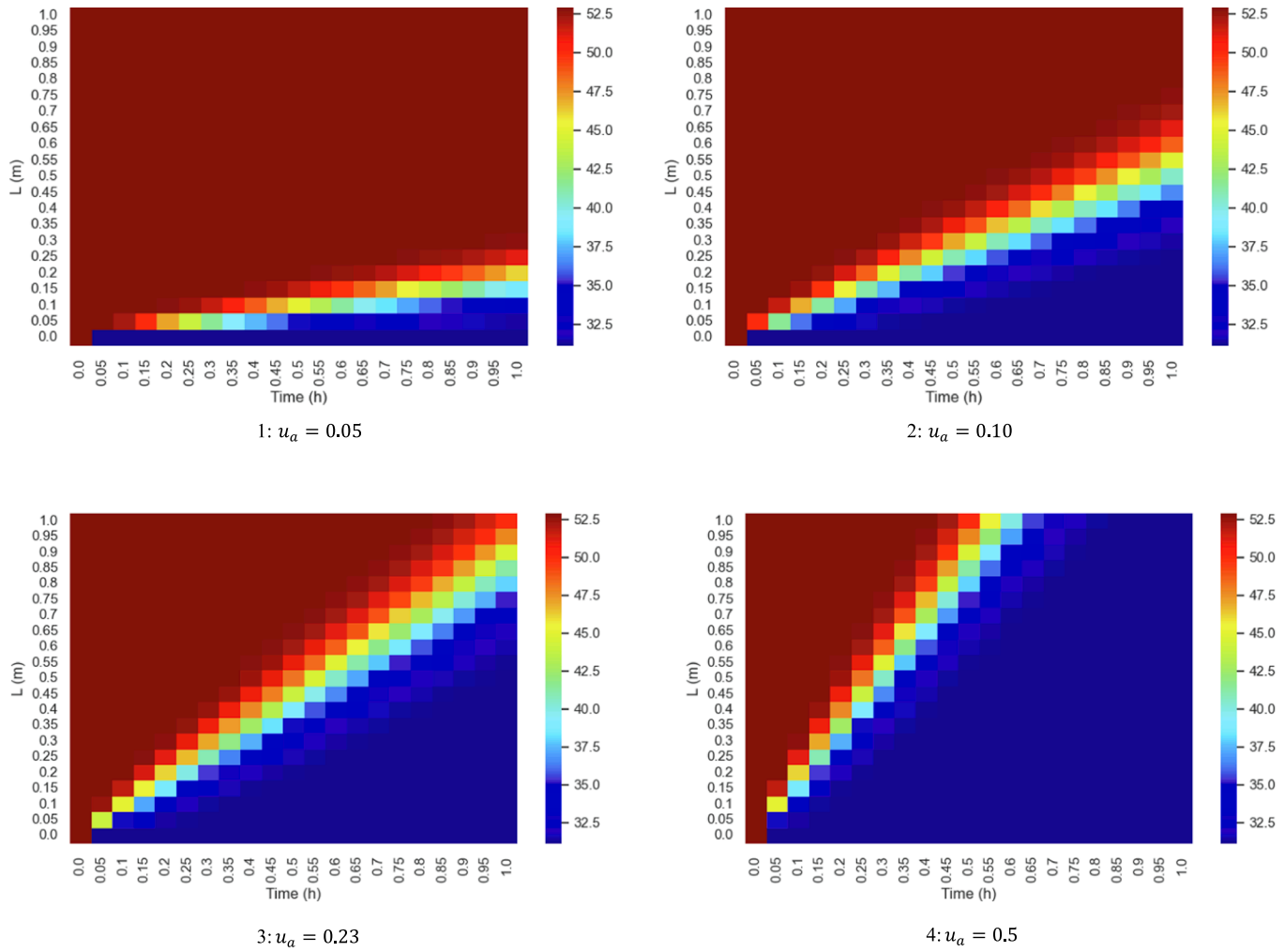

Fig. 5. Manufactured analytical solution proposed in this paper, varying the speed of the aeration air.

demonstrates satisfactory performance in addressing different velocities of the aeration air, as evidenced by the various parameter variations shown in Fig. 5.

5.4. Numerical verification

Results related to the discretization errors, effective order, and apparent order for temperature T at $y = L/2$ and $t = t_f/2$ are presented for the approximations used. The representative mesh size h was calculated as $h = \Delta y = \Delta t/2$ in the tests.

The behaviors of the discretization errors with mesh refinement for the methods used are shown in Fig. 6, where it can be observed that the discretization error decreased as the mesh size was refined for both methods studied (CDS-Crank-Nicolson and Leith). Furthermore, the curves have similar slopes, suggesting that these errors fall within the same order.

It is possible to see that the Leith scheme presents a smaller discretization error if compared to the CDS-Crank-Nicolson method.

Fig. 7 shows the effective (p_E) and apparent (p_U) orders with mesh refinement for each of the methods under study.

In Fig. 7, it can be observed that the effective (p_E) and apparent (p_U) orders of each method tend towards their asymptotic orders (p_L) presented in Table 1, which corroborates the validity of the numerical results.

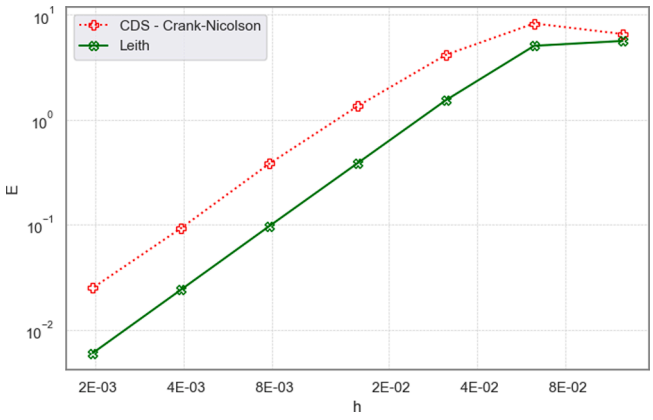

Fig. 6. Decay of discretization errors with mesh refinement.

6. Numerical experiments and discussions

Simulations were performed with space–time ratio $\lambda = 2, 4, 8$, 16 and 32 to compare the performance of the CDS-Crank-Nicolson and Leith's methods in two different aeration settings. In the following sections, the results obtained for $\lambda = 2$ and 32 in both settings are presented and discussed.

6.1. Setting A

The first setting, named setting A, involves a mass of soybeans 20 m high (L = 20 m) and initial and boundary temperatures given by T_I = 52.9 °C and T_B = 31.1 °C, respectively. A constant aeration air velocity of u_a = 0.10 m/s was applied for a duration of 40 h.

In order to compare the performance of the CDS-Crank-Nicolson and Leith's methods, simulations were performed for setting A with a space–time ratio λ = 32. Fig. 8 presents the temperature variation of soybeans under aeration forL_m = 10 m, which is in the middle of the storage location. Fig. 8.1 shows the temperature variation with respect to time, while Fig. 8.2 shows the numerical error between the numerical and analytical temperature for each point analyzed in Fig. 8.1. Fig. 8.3 displays the temperature variation throughout the storage location for t = 20 h, which is the mean time of aeration, and Fig. 8.4 shows the numerical error for each point analyzed in Fig. 8.3.

Fig. 9 displays the same graphs presented in Fig. 8, however, employing an space–time ratio λ = 2.

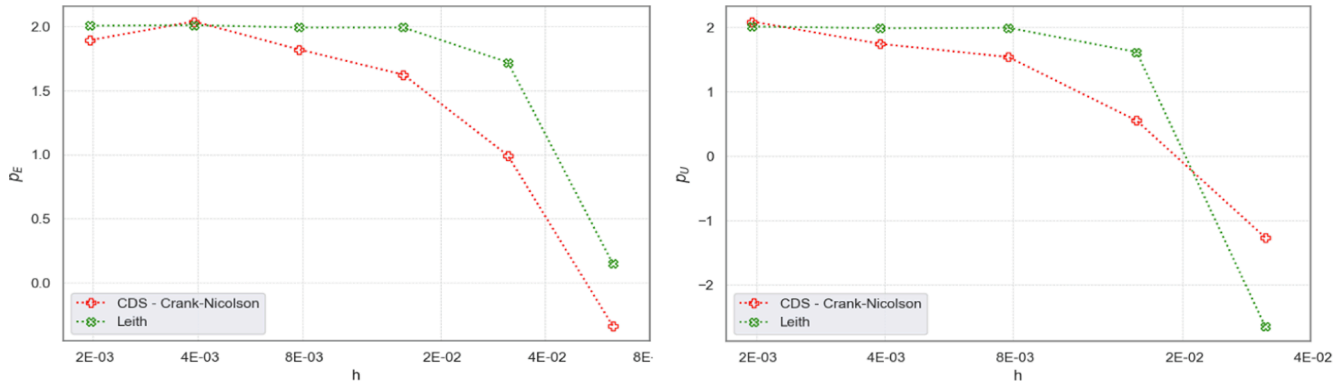

1: Effective Order

2: Apparent Order

Fig. 7. Behavior of the effective and apparent orders of discretization errors with mesh refinement for the methods under study.

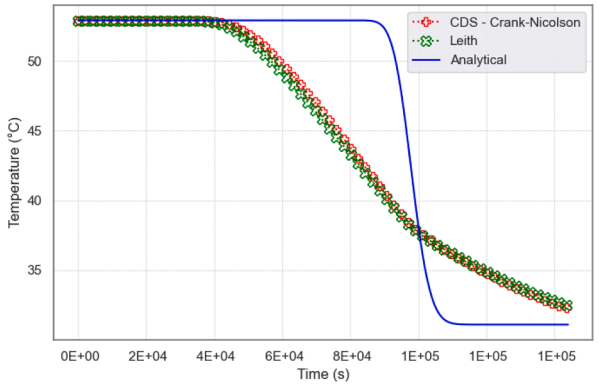

1: Temperature variation with respect to time for L_m = 10 m.

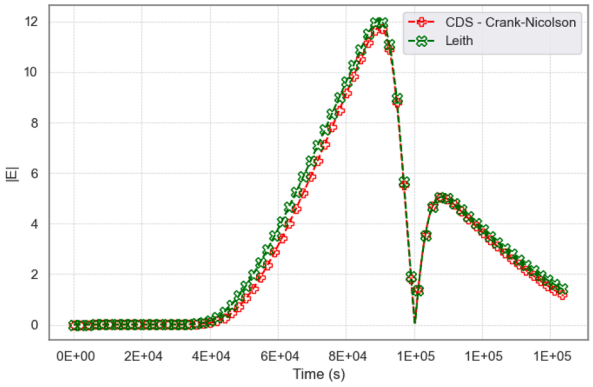

2: Numerical error of temperature *versus* time given by Fig 8.1.

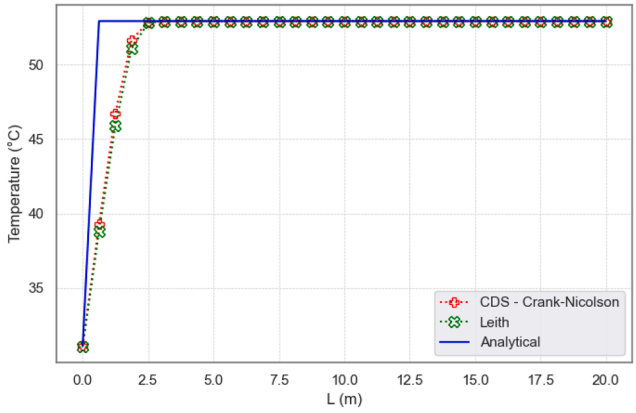

3: Temperature variation with respect to space for t = 20h.

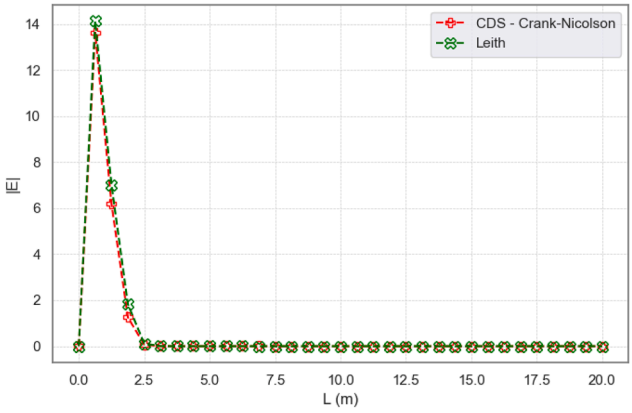

4: Numerical error of the temperature relative to space given by Fig 8.3.

Fig. 8. Grain temperature variations with λ = 32 in setting A.

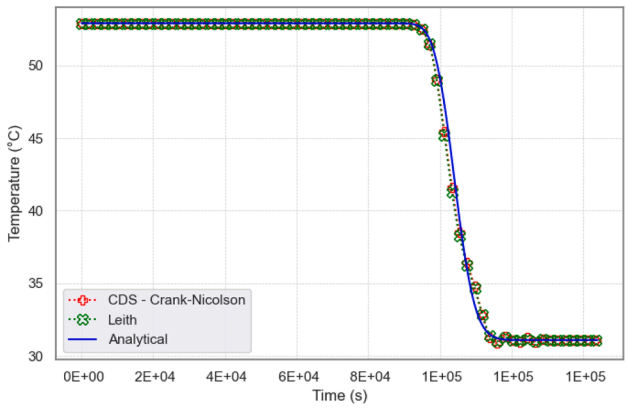

1: Temperature variation with respect to time for L_m= 10 m.

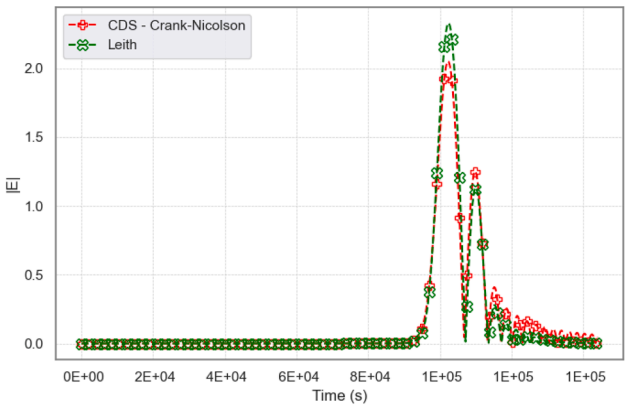

2: Numerical error of temperature *versus* time given by Fig 9.1.

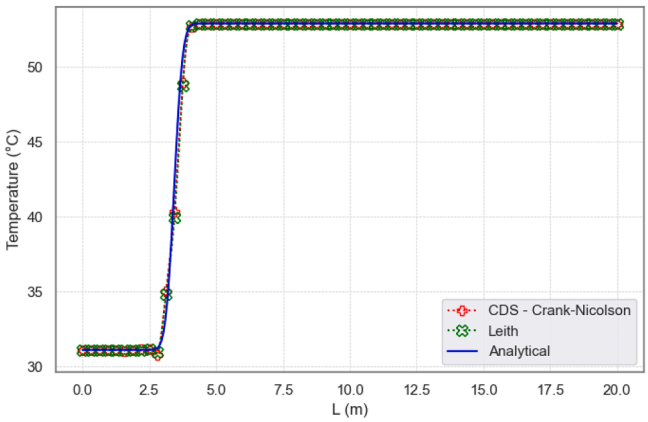

3: Temperature variation with respect to space for t = 20h.

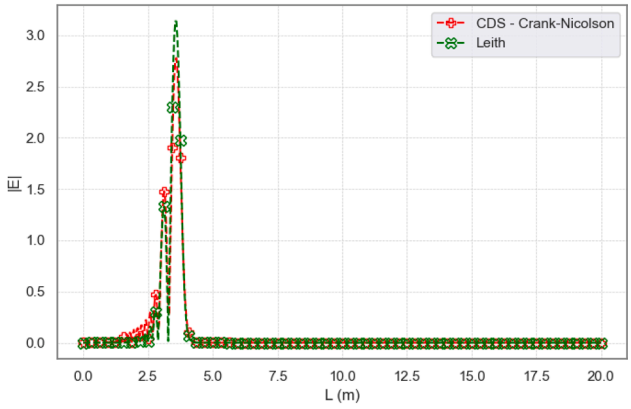

4: Numerical error of temperature relative to space given by Fig 9.3.

Fig. 9. Grain temperature variations with λ = 2 in setting A.

Using a high space–time ratio, such as λ = 32 (Fig. 8), the CDS-Crank-Nicolson and Leith's methods showed a clearly analogous performance. When using a low space–time ratio, as λ = 2 (Fig. 9), the CDS-Crank-Nicolson method evidenced a better performance, since the points of maximum numerical error, perceived in Figs. (9.2) and (9.4), are slightly smaller if compared to those obtained by the Leith's method.

That is, in setting A, when there is a high space–time ratio λ, the methods tend to perform similarly. When a low space–time ratio is employed, the CDS-Crank-Nicolson method provides slightly better results.

6.2. Setting B

The second setting, called setting B, corresponds to a mass of soybeans 35 m high (L = 35 m), T_I = 52.9 °C, T_B = 31.1 °C, and a constant aeration air velocity given byu_a = 0.20 m/s for 40 h. It can be noted that setting B consists of a larger storage location and a higher-capacity fan/motor system compared to setting A.

To compare the methods used, Fig. 10 presents the behavior of soybean temperature variation during aeration using a space–time ratio of λ = 32. Fig. 10.1 shows the variation of grain temperature over time for the middle point of the storage location (L_m = 17.5 m). Fig. 10.2 shows the numerical error (difference between numerical and analytical temperature) for each point analyzed in Fig. 10.1. Fig. 10.3 displays the variation of grain temperature across the storage location at the mean time of aeration (t = 20 h). Finally, Fig. 10.4 shows the numerical error of each point analyzed in Fig. 10.3. It is worth noting that setting B involves a larger storage location and higher aeration air velocity.

Fig. 11 displays the same graphs presented in Fig. 10, however, employing a space–time ratio λ = 2.

In setting B, when a high space–time ratio was used (λ = 32 in Fig. 10), both methods showed a similar performance, with a slight advantage for Leith's method. However, when a low space–time ratio was employed (λ = 2 in Fig. 11), the Leith's method provided better results, as the maximum numerical errors were significantly smaller compared to those obtained by the CDS-Crank-Nicolson method. This is clearly seen in Figs. (11.2) and (11.4).

In general, in setting B, independently of the space–time ratio, Leith's method shows a better performance in comparison with the CDS-Crank-Nicolson method. When employing a high space–time ratio, the methods tend to have a similar performance, however, in cases where a low space–time ratio is employed, Leith's method provides expressive results.

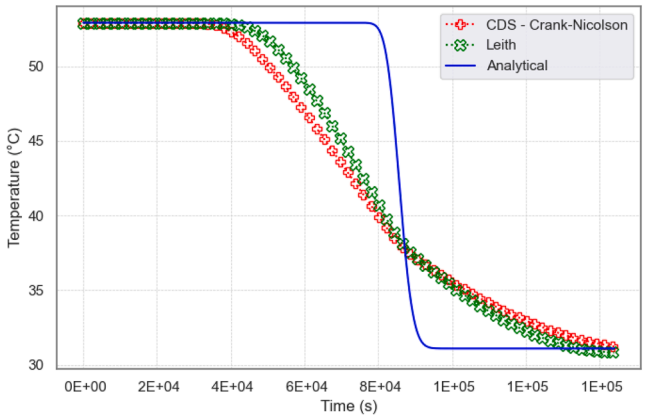

1: Temperature variation with respect to time for $L_m = 17.5\ m$. 17.5 m.

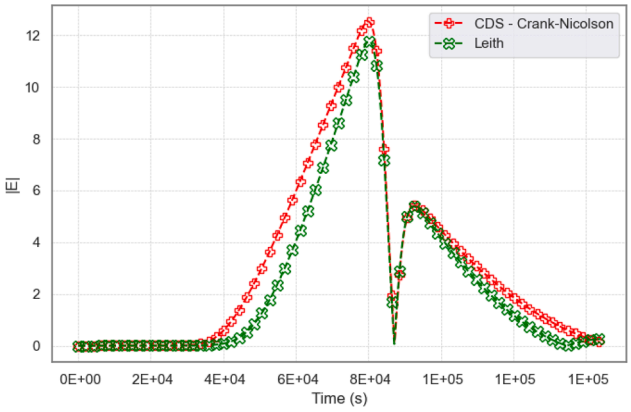

2: Numerical error of temperature versus time given by Fig 10.1.

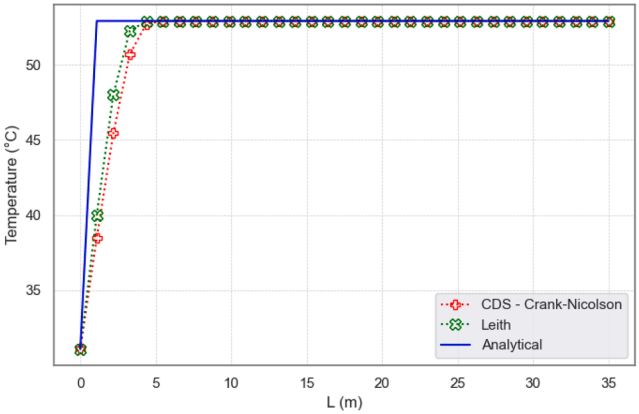

3: Temperature variation with respect to space for t = 20h.

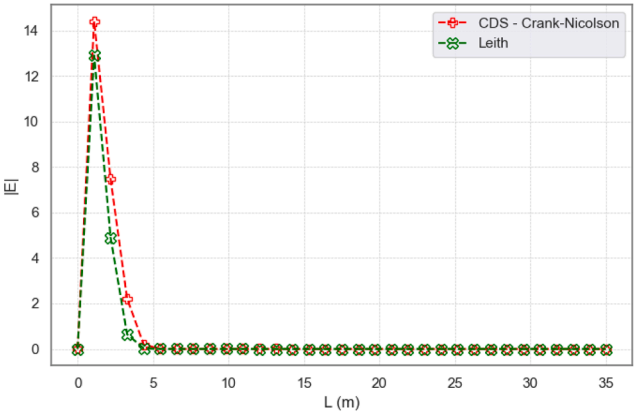

4: Numerical error of temperature versus space given by Fig 10.3.

Fig. 10. Grain temperature variations with λ = 32 in setting B.

6.3. *Discussions*

In setting A, where the storage location are smaller and the aeration air velocity is lower, the CDS-Crank-Nicolson method demonstrated a robust and satisfactory performance regardless of the space–time ratio, while the Leith's method showed similar behaviors only for problems with higher space–time ratio. On the other hand, in setting B, with larger storage location and higher aeration air velocity, Leith's method proved to be superior to the CDS-Crank-Nicolson method in all tested cases, including small space–time distortions meshes.

Moreover, given the small difference between the methods in setting A (Figs. 8 and 9) and the large difference in setting B (Figs. 10 and 11), Leith's method is demonstrated to be more efficient. These findings highlight the importance of considering the space–time ratio in numerical simulations of aeration in grain storage facilities and the potential benefits of using Leith's method in such settings.

The Leith's method has shown to be robust, efficient and stable, even when the space–time ratio is low. This indicates that the Leith's method can produce accurate and reliable results even when there are variations or uncertainties in the input parameters or conditions. Conversely, CDS-Crank-Nicolson may be more susceptible to changes in the input parameters, making it less reliable in certain situations. Thus, the Leith's method robustness makes it the preferred option for simulating aeration in grain storage systems, particularly in settings with larger storage location and higher aeration air velocities.

7. Conclusions

This paper introduces a new manufactured analytical solution using the MMS based on the work of Rigoni et al. (2022) for the mathematical model of grain mass aeration developed by Thorpe (2001b). The proposed solution is versatile and can handle various parameters related to soybean aeration. The FDM was employed to discretize the mathematical model, and the behavior of the CDS-Crank-Nicolson and Leith's methods regarding the space–time ratio was investigated. To avoid non-physical oscillations, artificial viscosity was introduced in the problem. Simulations were performed in different aeration settings using various space–time ratio. The Leith's method demonstrated higher efficiency and robustness than the CDS-Crank-Nicolson method. Therefore, the Leith's method is recommended for numerically solving the mathematical model of the aeration problem proposed by Thorpe.

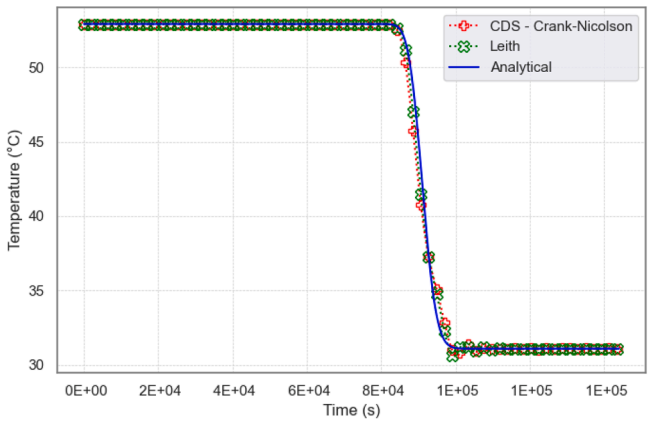

1: Temperature variation with respect to time for L_m = 17.5 m. 17.5 m.

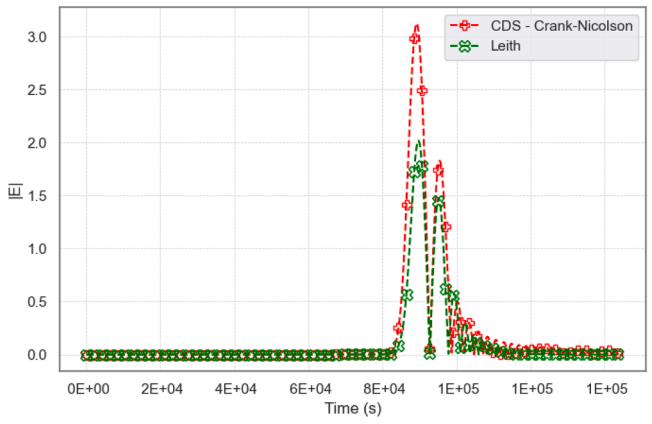

2: Numerical error of temperature *versus* time given by Fig. 11.1.

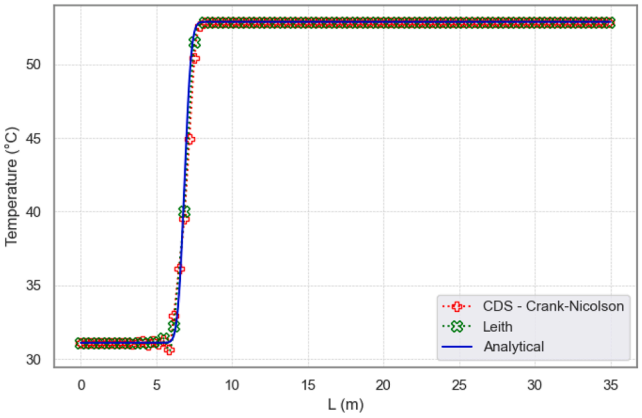

3: Temperature variation with respect to space for t = 20h.

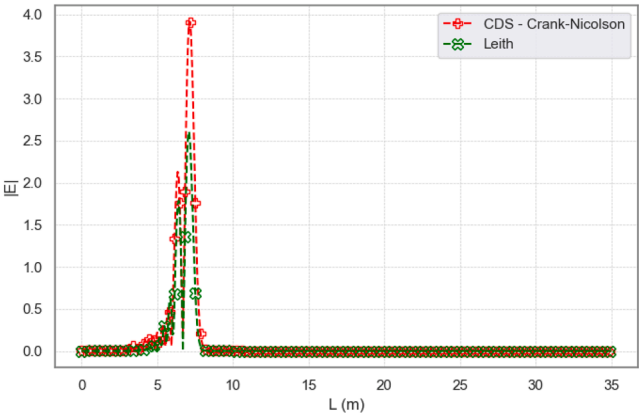

4: Numerical error of temperature relative to space given by Fig 11.3.

Fig. 11. Grain temperature variations with λ = 2 in setting B.

Declaration of Competing Interest

The authors declare that they have no known competing financial interests or personal relationships that could have appeared to influence the work reported in this paper.

Data availability

The data that has been used is confidential.

References

Alauzet, F., Loseille, A., 2016. A decade of progress on anisotropic mesh adaptation for computational fluid dynamics. Comput. Aided Des. 72, 13–39. https://doi.org/10.1016/j.cad.2015.09.005.

Brooker, D.B., Barker-Arkema, F.W., Hall, C.W., 1992. Drying and storage of grains and oilseeds. AVI Book Van Nostrand Reinhold.

Campbell, J., Vignjevic, R., 2009. Artificial Viscosity Methods for Modeling Shock Wave Propagation. In: Predictive Modeling of Dynamic Processes. Springer, US, Boston, MA, pp. 349–365. https://doi.org/10.1007/978-1-4419-0727-1_19.

Campbell, L.J., Yin, B., 2007. On the stability of alternating-direction explicit methods for advection-diffusion equations. Numerical Methods for Partial Differential Equations: An International Journal 23, 1429–1444. https://doi.org/10.1002/num.20233.

Canchun, J., Da-Wen, S., Chongwen, C., 2001. Computer simulation of temperature changes in a wheat storage bin. J. Stored Prod. Res. 37, 165–177. https://doi.org/10.1016/S0022-474X(00)00017-5.

Cañizares, L.D.C.C., da Silva Timm, N., Lang, G.H., Gaioso, C.A., Ferreira, C.D., de Oliveira, M., 2021. Effects of using wind exhausters on the quality and cost of soybean storage on a real scale. J. Stored Prod. Res. 93, 101834 https://doi.org/10.1016/j.jspr.2021.101834.

Chung, D., Pfost, H., 1967. Adsorption and Desorption of Water Vapor by Cereal Grains and Their Products Part I: Heat and Free Energy Changes of Adsorption and Desorption. Trans. ASABE 10, 549–551. https://doi.org/10.13031/2013.39726.

Coradi, P.C., de Oliveira, M.B., de Oliveira Carneiro, L., de Souza, G.A.C., Elias, M.C., Brackmann, A., Teodoro, P.E., 2020. Technological and sustainable strategies for reducing losses and maintaining the quality of soybean grains in real production scale storage units. J. Stored Prod. Res. 87, 101624 https://doi.org/10.1016/j.jspr.2020.101624.

Dehghan, M., 2005. Quasi-implicit and two-level explicit finite-difference procedures for solving the one-dimensional advection equation. Appl. Math Comput. 167, 46–67. https://doi.org/10.1016/j.amc.2004.06.067.

El Melki, M.N., El Moueddeb, K., Beyaz, A., 2022. Cooling Potential of Bin Stored Wheat by Summer and Autumn Aeration. Journal of Agricultural Sciences 28 (1), 145–158. https://doi.org/10.15832/ankutbd.715508.

FAO. (2020). *Food and Agriculture Organization of the United Nations.* Fonte: http://www.fao.org/publications/sofa/en/.

Ferreira, C., Ziegler, V., Goebel, J., Hoffmann, J., Carvalho, I., Chaves, F., 2019. Changes in phenolic acids and isoflavone contents during soybean drying and storage. J. Agric. Food Chem. 67 (4), 1146–1155. https://doi.org/10.1021/acs.jafc.8b06808.

Fleurat-Lessard, F., 2002. Qualitative reasoning and integrated management of the quality of stored grain: a promising new approach. J. Stored Prod. Res. 38, 191–218. https://doi.org/10.1016/S0022-474X(01)00022-4.

Hunter, A.J., 1987. An isostere equation for some common seeds. J. Agric. Eng. Res. 37, 93–105. https://doi.org/10.1016/S0021-8634(87)80008-2.

Jayas, D. S., & Cenkowski, S. (2006). Grain Property Values and Their Measurement. Em Handbook of industrial drying. Boca Raton: CRC Press. https://doi.org/10.1201/9781420017618.

Jayas, D.S., Muir, W.E., 2001. Aeration Systems Design. In: Navarro, E.S., Noyes, R. (Eds.), The mechanics and physics of modern grain aeration management. CRC Press, pp. 195–249.

Khatchatourian, O.A., Oliveira, F.A., 2006. Mathematical modeling of airflow and thermal state in large aerated grain storage. Biosyst. Eng. 95, 159–169. https://doi.org/10.1016/j.biosystemseng.2006.05.009.

Lax, P., Wendroff, B., 1960. Systems of conservation laws. Commun. Pure Appl. Math. 13, 217.

Leith, C.E., 1965. Numerical simulation of the earth's atmosphere. Methods Computational Physics 4, 1–28.

Lopes, D., & Neto, A. J. (2022). Zephyrus: Grain Aeration Strategy Based on the Prediction of Temperature and Moisture Fronts. Em *Information and Communication Technologies for Agriculture—Theme III: Decision* (Vol. 184). Springer Optimization and Its Applications. https://doi.org/10.1007/978-3-030-84152-2_9.

Lopes, D.C., Martins, J.H., Melo, E.C., Monteiro, P.M., 2006. Aeration simulation of stored grain under variable air ambient conditions. Postharvest Biol. Technol. 42, 115–120. https://doi.org/10.1016/j.postharvbio.2006.05.007.

Lopes, D.C., Neto, A.J., Santiago, J.K., 2014. Comparison of equilibrium and logarithmic models for grain drying. Biosyst. Eng. 118, 105–114. https://doi.org/10.1016/j.biosystemseng.2013.11.011.

Lopes, D.C., Neto, A.J., Júnior, R.V., 2015. Comparison of equilibrium models for grain aeration. J. Stored Prod. Res. 60, 11–18. https://doi.org/10.1016/j.jspr.2014.11.001.

Marchi, C.H., Martins, M.A., Novak, L.A., Araki, L.K., Pinto, M.A.V., Gonçalves, S.D.F.T., Moro, D.F., da Silva Freitas, I., 2016. Polynomial interpolation with repeated Richardson extrapolation to reduce discretization error in CFD. Appl. Math. Model. 40 (21–22), 8872–8885. https://doi.org/10.1016/j.apm.2016.05.029.

Melland, P., Albright, J., Urban, N.M., 2021. Differentiable programming for online training of a neural artificial viscosity function within a staggered grid Lagrangian hydrodynamics scheme. Machine Learning: Science and Technology 2, 025015. https://doi.org/10.1088/2632-2153/abd644.

Mousa, M.M., Ma, W.-X., 2020. Efficient modeling of shallow water equations using the method of lines and artificial viscosity. Mod. Phys. Lett. B 34, 2050051. https://doi.org/10.1142/S0217984920500517.

Navarro, S., Noyes, R.T., 2001. The mechanics and physics of modern grain aeration management. CRC Press.

Neumann, J.V., Richtmyer, R.D., 1950. A method for the numerical calculation of hydrodynamic shocks. J. Appl. Phys. 21, 232–237. https://doi.org/10.1063/1.1699639.

Nuttall, J.G., O'leary, G.J., Panozzo, J.F., Walker, C.K., Barlow, K.M., Fitzgerald, G.J., 2017. Models of grain quality in wheat—A review. Field Crops Res. 202, 136–145. https://doi.org/10.1016/j.fcr.2015.12.011.

Oberkampf, W.L., Blottner, F.G., 1998. Issues in Computational Fluid Dynamics Code Verification and Validation. AIAA J. 36, 687–695. https://doi.org/10.2514/2.456.

Oliveira, F., Khatchatourian, O.A., Bilhain, A., 2007. Thermal state of stored products in storage bins with aeration system: experimental-theoretical study. Engenharia Agrícola 27, 247–258.

Oliveira, F., Franco, S.R., Pinto, M.A.V., 2018. The effect of multigrid parameters in a 3D heat diffusion equation. Int. J. Appl. Mech. Eng. 23, 213–221. https://doi.org/10.1515/ijame-2018-0012.

Pfost, H. B., Rengifo, G. E., & Sauer, D. B. (1976). High temperature, high humidity grain storage. *ASAE, St. Joseph, MI*.

Rigoni, D., & Kwiatkowski Jr, J. E. (2020). Using the multigrid method to improve the performance of aeration process simulation. Proceeding Series of the Brazilian Society of Computational and Applied Mathematics, 7, 010331-1–010331-2.

Rigoni, D., Pinto, M.A., Kwiatkowski Jr., J.E., 2022. Verification and error analysis for the simulation of the grain mass aeration process using the method of manufactured solutions. Biosyst. Eng. 223 (1), 149–160. https://doi.org/10.1016/j.biosystemseng.2022.08.006.

Roache, P.J., 1998. Fundamentals of Computational Fluid Dynamics. Hermosa Publishers.

Roy, C.J., 2005. Review of code and solution verification procedures for computational simulation. J. Comput. Phys. 205, 131–156. https://doi.org/10.1016/j.jcp.2004.10.036.

Sinicio, R., Muir, W.E., Jayas, D.S., 1997. Sensitivity analysis of a mathematical model to simulate aeration of wheat stored in Brazil. Postharvest Biol. Technol. 11, 107–122. https://doi.org/10.1016/S0925-5214(97)00017-3.

Tannehill, J.C., Anderson, D.A., Pletcher, R.H., 1997. Computational Fluid Mechanics and Heat Transfer Vol. 2.

Thomas, L. H. (1949). Elliptic problems in linear difference equations over a network. *Watson Sci. Comput. Lab. Rept., Columbia University, New York, 1*, 71.

Thompson, T.L., 1972. Temporary storage of high-moisture shelled corn using continuous aeration. Trans. ASAE 15, 333–0337. https://doi.org/10.13031/2013.37900.

Thompson, T., Peart, R., Foster, G., 1968. Mathematical simulation of corn drying a new model. Trans. ASAE 11, 582–586.

Thorpe, G.R., 2001a. Ambient Air Properties in Aeration. In: Em *The Mechanics and Physics of Modern Grain Aeration Management*. CRC Press, pp. 79–120.

Thorpe, G. R. (2001). Physical basic of aeration. *In: S. Navarro, R. T. Noyes, The Mechanics and Physics of Modern Grain Aeration Management, 1*, 125-185.

Van Genuchten, M. T., Service, U. S., & Alves, W. J. (1982). *Analytical Solutions of the One-dimensional Convective-dispersive Solute Transport Equation.* U.S. Department of Agriculture, Agricultural Research Service.

Xuana, G., Zheng, H., Xiaoyu, S., et al., 2017. A Two-dimensional lattice Boltzmann method for compressible flows. Acta Informatica Malaysia (AIM) 1, 32–35.

Ziegler, V., Vanier, N.L., Ferreira, C.D., Paraginski, R.T., Monks, J.L.F., Elias, M.C., 2016. Changes in the Bioactive Compounds Content of Soybean as a Function of Grain Moisture Content and Temperature during Long-Term Storage. J. Food Sci. 81 (3), H762–H768. https://doi.org/10.1111/1750-3841.13222.